

## Polyynes

Deutsche Ausgabe: DOI: 10.1002/ange.201608633  
Internationale Ausgabe: DOI: 10.1002/anie.201608633

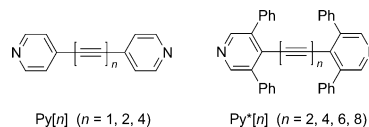
## Pyridyl-Endcapped Polyynes: Stabilized Wire-like Molecules

Maximilian Krempe, Rainer Lippert, Frank Hampel, Ivana Ivanović-Burmazović, Norbert Jux, and Rik R. Tykwinski\*

**Abstract:** A 4-ethynylpyridyl derivative with sterically shielding phenyl groups in the 3- and 5-positions has been synthesized and used to terminate a series of polyynes. This approach allows for the synthesis of stable polyynes up to an octayne, twice as long as previous accessible for “unstabilized” pyridyl-endcapped polyynes. The potential of these polyynes as wire-like linkers to metal centers is demonstrated by axial coordination of pyridyl groups to zinc- and ruthenium-metalloporphyrins.

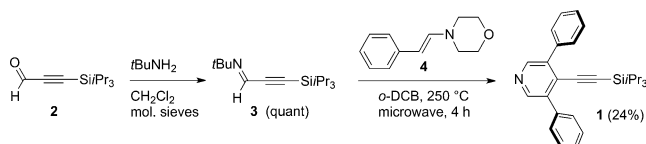
Molecular wires typically feature a rigid, conjugated structure that can facilitate electron transport. In the ongoing quest to miniaturize devices, it is expected that wire-like molecules could serve as a fundamental building block for molecular electronics.<sup>[1,2]</sup> The Lewis basicity of pyridyl nitrogen, i.e., its ligand properties, allows the design and synthesis of molecules for supramolecular and materials chemistry (e.g., nanoobjects,<sup>[3]</sup> coordination polymers,<sup>[4]</sup> MOFs,<sup>[5]</sup> semiconducting materials,<sup>[6]</sup> light harvesting<sup>[7]</sup>). Pyridyl groups also provide an opportunity to link to metal electrodes, such as gold, furnishing molecular wires.<sup>[8]</sup> As a conjugated linker between terminal pyridyl groups, polyynes offer attractive characteristics. Namely, the sp-hybridized  $\pi$ -system of polyynes is nearly cylindrical and therefore, the influence of molecular rotation is limited.<sup>[9,10a]</sup> Unfortunately, functionalized polyyne derivatives are often kinetically labile, limiting their usefulness.<sup>[10,11]</sup> To the best of our knowledge, there are no known stable polyynes that incorporate pyridyl anchoring groups and consist of more than four C–C triple bonds (i.e., a tetrayne).<sup>[9,12]</sup> As result, opportunities to study the wire-like properties of polyynes as a function of length are quite limited, albeit very desirable.<sup>[13]</sup>

Herein we report a stabilization Scheme for pyridyl polyynes, through the development of 4-ethynyl-3,5-diphe-



nylpyridine as a sterically encumbered endgroup that can be used for the assembly of polyynes Py\*[n], including the di-, tetra-, hexa-, and octaynes ( $n = 2, 4, 6, 8$ , respectively). The hexa- and octayne are the longest stable pyridyl endcapped polyynes reported to date.<sup>[14]</sup> The potential of Py\*[n] polyynes to bind to metals is demonstrated through axial coordination to metalloporphyrins. The electronic absorption and electrochemical properties, as well as the stability and solid-state structure of the supramolecular porphyrin–polyyne conjugates are described.

The synthesis of 4-ethynyl pyridine **1** was envisioned based on a procedure reported by Komatsu et al.<sup>[15]</sup> Thus, the reaction of propargyl aldehyde **2** with *tert*-butylamine gave the corresponding imine **3** in quantitative yield.<sup>[16]</sup> Condensation of **3** with enamine **4**<sup>[17]</sup> in *o*-dichlorobenzene under microwave irradiation gave the ethynyl pyridine **1** in moderate yield (24%, Scheme 1). Attempts to optimize this reaction via temperature and reaction time variation did not effectively increase the product yield.



**Scheme 1.** Synthesis 4-ethynylpyridine derivative **1**.

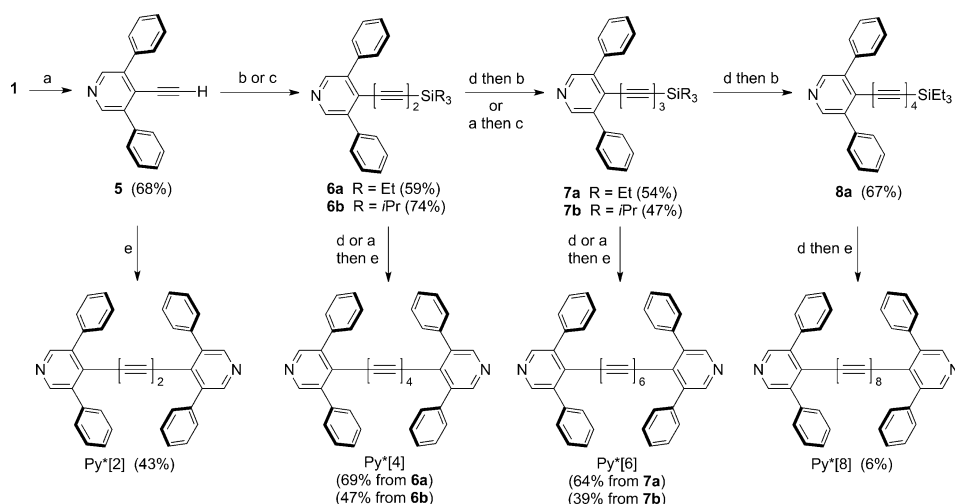
With compound **1** in hand, a sequence of desilylation and oxidative coupling was used to form elongated pyridyl-endcapped polyynes Py\*[n] ( $n = 2, 4, 6, 8$ ), as shown in Scheme 2. Desilylation of **1** with tetrabutylammonium fluoride (TBAF) gave the terminal alkyne **5** as a colorless crystalline solid. Cross-coupling of **5** with either bromoethynyl triethylsilane (**9**)<sup>[18]</sup> or bromoethynyl triisopropylsilane (**10**)<sup>[19]</sup> under Cadiot–Chodkiewicz heterocoupling conditions<sup>[20]</sup> gave diynes **6a** and **6b** in 59% and 74% yield, respectively. Desilylation of diynes **6a** and **6b** with CsF or TBAF, respectively, gave the terminal butadiyne, which was stable in solution, but rapidly decomposed in the solid state. Thus, working in solution, coupling with either **9** or **10** gave the corresponding TES- and TIPS-hexatriynes (**7a** and **7b**, respectively) as stable brown oils. Attempts to form octate-

[\*] M. Krempe, Dr. F. Hampel, Prof. Dr. N. Jux, Prof. Dr. R. R. Tykwinski  
Department of Chemistry and Pharmacy &  
Interdisciplinary Center for Molecular Materials (ICMM)  
University of Erlangen–Nürnberg (FAU) (Germany)  
E-mail: rik.tykwinski@fau.de  
Homepage: <http://www.chemie.uni-erlangen.de/tykwinski>

Dr. R. Lippert, Prof. Dr. I. Ivanović-Burmazović  
Department of Chemistry and Pharmacy  
Chair of Bioinorganic Chemistry  
University of Erlangen–Nürnberg (FAU) (Germany)

Prof. Dr. R. R. Tykwinski  
Current address:  
Department of Chemistry, University of Alberta  
Edmonton, Alberta T6G 2G2 (Canada)  
E-mail: rik.tykwinski@ualberta.ca

Supporting information for this article can be found under:  
<http://dx.doi.org/10.1002/ange.201608633>.



**Scheme 2.** Synthesis of pyridyl endcapped polyynes  $\text{Py}^*[n]$ . Reagents and conditions: a)  $\text{R} = i\text{Pr}$ : TBAF, THF/ $\text{H}_2\text{O}$ , RT; b)  $\text{CuCl}$ ,  $\text{NH}_2\text{OH}\cdot\text{HCl}$ ,  $n\text{PrNH}_2$ ,  $\text{CH}_2\text{Cl}_2$  or EtOH,  $\text{Br-CC-SiEt}_3$  (**9**),  $0^\circ\text{C}$  to RT; c)  $\text{CuCl}$ ,  $\text{NH}_2\text{OH}\cdot\text{HCl}$ ,  $n\text{PrNH}_2$ ,  $\text{CH}_2\text{Cl}_2$  or EtOH,  $\text{Br-CC-SiPr}_3$  (**10**),  $0^\circ\text{C}$  to RT; d)  $\text{R} = \text{Et}$ :  $\text{CsF}$ , THF/ $\text{H}_2\text{O}$ , RT; e)  $\text{CuCl}$ , TMEDA, acetone or  $\text{CH}_2\text{Cl}_2$ , RT.

trayne **8a** starting from **7b** were unsuccessful. On the other hand, desilylation of **7a** using  $\text{CsF}$  could be accomplished, as has been successful for other fluoride sensitive polyynes.<sup>[11a]</sup> The resulting terminal triyne was not stable to isolation, as was quickly carried on to the coupling reaction with bromoalkyne **9**, giving TES-octatetrayne **8a** as a stable brown oil in a respectable yield of 67%. Frustratingly, all attempts to subject **8a** to the analogous sequence of desilylation/heterocoupling steps have not been successful.

With polyynes **5–8** in hand, the formation of the pyridyl endcapped polyynes  $\text{Py}^*[n]$  was developed. Terminal alkyne **5** was subjected to homocoupling under Hay conditions<sup>[21]</sup> to give  $\text{Py}^*[2]$  in a yield of 43%. The use of modified Eglinton–Galbraith coupling conditions ( $\text{Cu}(\text{OAc})_2$  in 2,6-lutidine) did not lead to the desired product.<sup>[11a,22]</sup> The moderate yield of  $\text{Py}^*[2]$  is likely due to steric demands of the pyridyl endgroup, as significant amounts of starting material **5** were recovered. Desilylation of diyne **6a** and Hay coupling gave  $\text{Py}^*[4]$  as a yellow solid in 69% yield, while starting with **6b** gave lower yield of  $\text{Py}^*[4]$ . The analogous sequence of desilylation and homocoupling gave  $\text{Py}^*[6]$  as a greenish solid in 64% yield from **7a**, while starting from **7b** gave only 39% yield; to our knowledge, this is the first synthesis of an isolable pyridyl endcapped hexayne.<sup>[14]</sup> Finally, octayne  $\text{Py}^*[8]$  was formed from **8a** by careful desilylation and homocoupling, and it was isolated as a red solid in low yield (6%). The octayne was stable under ambient conditions, and could be stored for several weeks when kept under refrigeration.

As analyzed by differential scanning calorimetry (DSC), diyne  $\text{Py}^*[2]$  shows a melting point (mp.) at  $193^\circ\text{C}$ , and is stable as a liquid until decomposition (dp.) at  $314^\circ\text{C}$ . Given the tendency of diarylbutadiynes to react at elevated temperature, the stability of  $\text{Py}^*[2]$  in the liquid phase at elevated temperatures is an excellent indication of the ability of the 3,5-diphenylpyridyl groups to shield the normally reactive butadiyne core.  $\text{Py}^*[2]$  is also significantly more stable than  $\text{Py}[2]$ , which shows a mp of  $207^\circ\text{C}$ , followed quickly by

decomposition at  $209^\circ\text{C}$  (see Figure S19). Tetrayne  $\text{Py}^*[4]$  shows no melting point and decomposes at  $235^\circ\text{C}$ , which is significantly higher than that of  $\text{Py}[4]$  (dp.  $160^\circ\text{C}$ ).<sup>[23]</sup> The longest derivatives,  $\text{Py}^*[6]$ , and  $\text{Py}^*[8]$ , likewise show only decomposition points, at  $178^\circ\text{C}$  and  $163\text{--}165^\circ\text{C}$ , respectively.<sup>[24]</sup>

Broad absorption bands are found in the UV-vis spectrum of  $\text{Py}^*[2]$ , while the longer polyynes,  $\text{Py}^*[4]$ ,  $\text{Py}^*[6]$ , and  $\text{Py}^*[8]$ , spectra display patterns with vibronic fine structure consistent with other polyynes (Figure 1), such as those endcapped with 4-pyridyl ( $\text{Py}[n]$ ) or phenyl groups ( $\text{Ph}[\text{CC}]_n\text{-Ph}$ ).

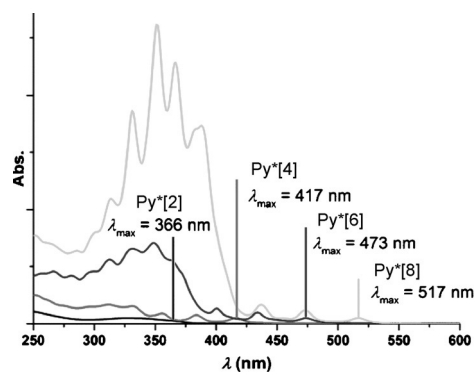
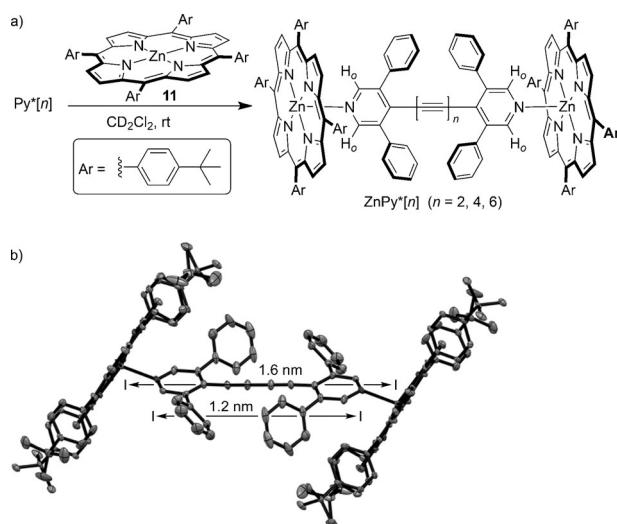


**Figure 1.** UV-vis spectra of  $\text{Py}^*[n]$  ( $n = 2, 4, 6, 8$ ) in  $\text{CH}_2\text{Cl}_2$  solutions. To facilitate comparison, the absorbance values are normalized to that of  $\lambda_{\text{max}}$  (for quantitative UV-vis spectra of  $\text{Py}^*[n]$  ( $n = 2, 4, 6$ ), see Figure S1).

$\text{Ph}[n]$ ). The nature of the aryl endgroup has a noticeable effect on  $\lambda_{\text{max}}$  values for shorter polyynes, e.g., there is a range of 38 nm in structurally similar diynes  $\text{Ph}[2]$  ( $\lambda_{\text{max}} = 328\text{ nm}$  in THF),<sup>[25]</sup>  $\text{Py}[2]$  ( $\lambda_{\text{max}} = 330\text{ nm}$  in  $\text{CHCl}_3$ ),<sup>[26]</sup>  $\text{Py}^*[2]$  ( $\lambda_{\text{max}} = 366\text{ nm}$  in  $\text{CH}_2\text{Cl}_2$ ). The endgroup effect diminishes for longer derivatives, and essentially disappears for octaynes  $\text{Py}^*[8]$  and  $\text{Ph}[8]$ <sup>[25]</sup> with  $\lambda_{\text{max}} = 517$  and  $512\text{ nm}$  (in  $\text{CH}_2\text{Cl}_2$  and THF, respectively). The UV-vis spectra of polyynes  $\text{Py}^*[n]$  show no appreciable solvatochromism (see Figure S2), although protonation by acid (e.g., TFA) results in a redshift of  $\lambda_{\text{max}}$  ( $\text{Py}^*[6]$  473 nm,  $\text{Py}^*[6]\text{H}^+$  488 nm, in  $\text{CH}_2\text{Cl}_2$ ), due to lowering of the LUMO level by the electron withdrawing effect on the pyridinium moiety of  $\text{Py}^*[6]\text{H}^+$  (the process is completely reversible through the addition of base, see Figure S3).

The ability of  $\text{Py}^*[n]$  to bridge two metals was initially explored by axial coordination to a Zn-metalloporphyrin.<sup>[27]</sup> The self-assembly reactions of  $\text{Py}^*[2]$ ,  $\text{Py}^*[4]$ , and  $\text{Py}^*[6]$  with porphyrin **11**<sup>[28]</sup> were performed by titration of the porphyrin

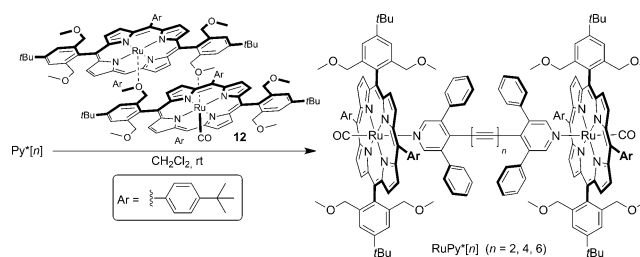
to the respective polyynes in  $\text{CD}_2\text{Cl}_2$  solution. The reactions were monitored by  $^1\text{H}$  NMR spectroscopy and resulted in essentially quantitative formation of  $\text{ZnPy}^*[2]$ ,  $\text{ZnPy}^*[4]$ , and  $\text{ZnPy}^*[6]$ .<sup>[29]</sup> Complexes  $\text{ZnPy}^*[n]$  were, unfortunately, not particularly soluble in typical organic solvents, but their formation could be conclusively established through a combination of  $^1\text{H}$ , COSY, and HSQC NMR experiments, as well as ESI MS. In particular, the proximity of the pyridyl moiety of the polyynes to the aromatic porphyrin core leads to a substantial upfield shift of the signal for the *ortho* protons ( $\text{H}_o$ , Scheme 3a), from ca.  $\delta$  8.60 in polyynes  $\text{Py}^*[n]$  to  $\delta$  4.12 ( $\text{ZnPy}^*[2]$ ), 4.64 ( $\text{ZnPy}^*[4]$ ), and 4.60 ( $\text{ZnPy}^*[6]$ ) in supramolecular complexes  $\text{ZnPy}^*[n]$  (see the Supporting Information for details). Crystallographic analysis of  $\text{ZnPy}^*[2]$  (Scheme 3b) outlines the dimensions of the polyynes, which spans 1.2 nm (N to N) and 1.6 nm (Zn to Zn). The two pyridyl rings are essentially coplanar (torsion angle of  $5^\circ$ ), but there is a slight distortion of the structure with respect to the angle between planes of the porphyrin and the pyridyl ring ( $62^\circ$ ).



**Scheme 3.** a) Synthesis of porphyrin-encapped pyridyl polyynes  $\text{ZnPy}^*[n]$ . b) X-ray crystallographic structure of  $\text{ZnPy}^*[2]$  in the solid state (ellipsoids drawn at the 30% probability level; hydrogen atoms have been omitted for clarity).

The limited solubility of the  $\text{ZnPy}^*[n]$  complexes directed efforts to complexes formed from tetraaryl Ru-porphyrin **12**.<sup>[30,31]</sup> Thus, combining the appropriate polyynes  $\text{Py}^*[n]$  ( $n = 2, 4$ , and  $6$ ) with **12** in  $\text{CH}_2\text{Cl}_2$ , followed by purification via column chromatography, gave a series of complexes endcapped with Ru-porphyrins (Scheme 4). The products  $\text{RuPy}^*[n]$  ( $n = 2, 4$ , and  $6$ ) showed good solubility in chlorinated solvents, and the structures were confirmed through a combination of NMR spectroscopy and mass spectrometry. In particular, the characteristic upfield shifts of the pyridyl protons were indicative of axial coordination to the porphyrin (see the Supporting Information for NMR spectra).

The supramolecular complexes  $\text{RuPy}^*[4]$  and  $\text{RuPy}^*[6]$  show remarkable thermal stability, with decomposition onset temperatures of 248 and  $232^\circ\text{C}$ , respectively, as measured by DSC. Thus, the thermal stability of  $\text{RuPy}^*[4]$  and  $\text{RuPy}^*[6]$  is



**Scheme 4.** Synthesis of Ru-porphyrin-encapped pyridyl polyynes  $\text{RuPy}^*[n]$  (yields are quantitative).

actually greater than that of the respective polyynes precursors  $\text{Py}^*[4]$  ( $235^\circ\text{C}$ ) and  $\text{Py}^*[6]$  ( $178^\circ\text{C}$ ). The similar decomposition temperatures and DSC profiles for  $\text{RuPy}^*[4]$  and  $\text{RuPy}^*[6]$  suggest that decomposition initiates by dissociation of the polyynes from the porphyrin endgroup. Thus, it is noteworthy that supramolecular self-assembly presents itself as a means to increase polyynes stability, especially when coupled with sterically demanding endgroups as found in polyynes  $\text{Py}^*[n]$ .

The UV-vis absorption spectra of both series  $\text{ZnPy}^*[n]$  and  $\text{RuPy}^*[n]$  are, for the most part, the sum of their component parts (i.e.,  $\text{Py}^*[n]$  + 2 equiv of porphyrin), which gives little indication of the ability of the polyynes to mediate electronic coupling between metals (see Figures S6 and S7). As a result, electrochemical methods (cyclic and differential pulse voltammetry, CV and DPV, respectively) have been used to study the more soluble  $\text{RuPy}^*[n]$  series, in comparison to polyynes  $\text{Py}^*[n]$  (see the Supporting Information for voltammograms). The redox properties of polyynes have only been rarely investigated, but it is known that the electron-deficient nature of a polyynes dictates the electronic makeup.<sup>[32,33]</sup> Consistent with this, no oxidation event is observed for  $\text{Py}^*[n]$  polyynes within the accessible potential window (see Tables 1 and S1) whereas DP voltammograms show a reduction that becomes easier as a function of increasing length from  $\text{Py}^*[2]$ , to  $\text{Py}^*[4]$ , and finally  $\text{Py}^*[6]$  ( $-1.49$  V,  $-1.21$  V, and  $-1.03$  V, respectively). The reduction potentials reflect a lowering of the LUMO energy<sup>[34]</sup> and are consistent with decreasing HOMO–LUMO gap ( $E_{\text{g,opt}}$ ) as

**Table 1:** Electrochemical<sup>[a]</sup> and optical data for  $\text{Py}^*[n]$ , **12**, and  $\text{RuPy}^*[n]$ .

Compound	$E_{\text{red1}}$ [V]	$E_{\text{ox1}}$ [V]	$E_{\text{ox2}}$ [V]	$\lambda_{\text{max}}^{[b]}$ [nm]	$E_{\text{g,opt}}^{[c]}$ [eV]
$\text{Py}^*[2]$	$-1.49$	–	–	366	3.24
$\text{Py}^*[4]$	$-1.21$	–	–	417	2.88
$\text{Py}^*[6]$	$-1.03$	–	–	473	2.55
$\text{Py}^*[8]$	[d]	[d]	[d]	517	2.33
<b>12</b>	$-1.58$	0.84	1.22	563	2.06
$\text{RuPy}^*[2]$	$-1.45$	0.92	1.49	568	2.09
$\text{RuPy}^*[4]$	$-1.28$	0.91	1.56	567	2.09
$\text{RuPy}^*[6]$	$-1.03$	0.91	N/A	568	2.07

[a] Differential pulse voltammetry in  $\text{CH}_2\text{Cl}_2$  solutions with Ag/AgCl couple as reference (see the Supporting Information for voltammograms). [b] Based on UV-vis spectral analysis of  $\text{CH}_2\text{Cl}_2$  solution. [c] Estimated optical band gap from solution state UV-vis spectra

(estimated from the intercept of a tangent line applied to the lower edge of  $\lambda_{\text{max}}$  with the x-axis). [d] Not measured.



a function of increasing polyyn length (Table 1). The first oxidation potential of complexes RuPy\*[*n*] ( $E_{\text{ox1}} \approx 0.9$  V) is slightly more difficult in comparison to model compound **12** ( $E_{\text{ox1}} \approx 0.8$  V), which reflects the electron withdrawing character of the Py\*[*n*] spacer that renders the Ru-porphyrin more electron deficient. While the length of the Py\*[*n*] spacer has no impact on  $E_{\text{ox1}}$ , the second oxidation event ( $E_{\text{ox2}}$ ) increases from RuPy\*[2] (1.49 V) to RuPy\*[4] (1.56 V); the second oxidation of RuPy\*[6] is not observed (seemingly due to decomposition of material during measurement). The first reduction potentials ( $E_{\text{red1}}$ ) of RuPy\*[*n*] are comparable to those of the “naked” polyynes Py\*[*n*]. Thus, electrochemical characterization suggests that porphyrin **12** and Py\*[*n*] behave essentially independently, with oxidation occurring at the porphyrin and reduction at the polyyn. This behavior is in direct contrast to that of mixed-valence ionic states reported for diruthenium<sup>[35]</sup> and Pt<sup>II</sup> acetylide complexes.<sup>[33]</sup>

In summary, the synthesis and characterization of pyridyl endcapped oligoynes with unprecedented length is reported, in which steric shielding from the endgroups provides a significant stabilization effect for the acetylenic framework. Using Py\*[*n*] polyynes, supramolecular complexes are formed by axial coordination to Zn- and Ru-porphyrins. Single crystal X-ray analysis of the complex ZnPy\*[2] defines the desired sandwich-like binding behavior, as well as a planar conformation of the pyridyl endgroups. Electrochemical analysis of Py\*[*n*] (*n* = 2, 4, 6) outlines an increasingly facile reduction as a function of increasing length, while the redox behavior of complexes RuPy\*[*n*] (*n* = 2, 4, 6) indicates polyyn-centered reduction and porphyrin-centered oxidation. Finally, the presence of the Ru-porphyrin in RuPy\*[*n*] further enhances thermal stability, in comparison to the naked analogous polyyn Py\*[*n*].

## Acknowledgments

We are grateful for funding from the University of Erlangen–Nürnberg, the Deutsche Forschungsgemeinschaft (SFB 953, “Synthetic Carbon Allotropes”). We thank Dr. Elena Klimkina for her help concerning NMR spectroscopy, and Jacqueline Krempe for help with the table of contents graphic. R.L. and I.I.-B gratefully acknowledge support through the “Solar Technologies Go Hybrid” initiative of the State of Bavaria.

**Keywords:** electrochemistry · ethynyl pyridines · molecular wires · polyynes · porphyrins

**How to cite:** *Angew. Chem. Int. Ed.* **2016**, 55, 14802–14806  
*Angew. Chem.* **2016**, 128, 15022–15026

- [1] L. A. Bumm, J. J. Arnold, M. T. Cygan, T. D. Dunbar, T. P. Burgin, L. Jones II, D. L. Allara, J. M. Tour, P. S. Weiss, *Science* **1996**, 271, 1705–1707.
- [2] D. M. Guldi, H. Nishihara, L. Venkataraman, *Chem. Soc. Rev.* **2015**, 44, 842–844.
- [3] a) R. Chakrabarty, P. S. Mukherjee, P. J. Stang, *Chem. Rev.* **2011**, 111, 6810–6918; b) T. R. Cook, Y.-R. Zheng, P. J. Stang, *Chem. Rev.* **2013**, 113, 734–777.
- [4] N. N. Adarsh, P. Dastidar, *Chem. Soc. Rev.* **2012**, 41, 3039–3060.
- [5] N. C. Burtch, K. S. Walton, *Acc. Chem. Res.* **2015**, 48, 2850–2857.
- [6] Y. Z. Wang, A. J. Epstein, *Acc. Chem. Res.* **1999**, 32, 217–224.
- [7] G. Bottari, G. de la Torre, D. M. Guldi, T. Torres, *Chem. Rev.* **2010**, 110, 6768–6818; L. Zhang, J. M. Cole, *ACS Appl. Mater. Interfaces* **2015**, 7, 3427–3455.
- [8] E. Leary, A. La Rosa, M. T. González, G. Rubio-Bollinger, N. Agraït, N. Martín, *Chem. Soc. Rev.* **2015**, 44, 920–942.
- [9] a) M. Gulcur, P. Moreno-García, X. Zhao, M. Baghernejad, A. S. Batsanov, W. Hong, M. R. Bryce, T. Wandlowski, *Chem. Eur. J.* **2014**, 20, 4653–4660; b) P. Moreno-García, M. Gulcur, D. Z. Manrique, T. Pope, W. Hong, V. Kaliginedi, C. Huang, A. S. Batsanov, M. R. Bryce, C. Lambert, T. Wandlowski, *J. Am. Chem. Soc.* **2013**, 135, 12228–12240.
- [10] a) C. Wang, A. S. Batsanov, M. R. Bryce, S. Martín, R. J. Nichols, S. J. Higgins, V. M. García-Suárez, C. J. Lambert, *J. Am. Chem. Soc.* **2009**, 131, 15647–15654; b) C. Wang, H. Jia, T. Li, Y. Wang, *Jilin Huagong Xueyuan Xuebao* **2012**, 20, 33–36.
- [11] a) W. A. Chalifoux, R. R. Tykwinski, *Nat. Chem.* **2010**, 2, 967–971; b) L. D. Movsisyan, M. Franz, F. Hampel, A. L. Thompson, R. R. Tykwinski, H. L. Anderson, *J. Am. Chem. Soc.* **2016**, 138, 1366–1376.
- [12] S. Ballmann, W. Hieringer, D. Secker, Q. Zheng, J. A. Gladysz, A. Görling, H. B. Weber, *ChemPhysChem* **2010**, 11, 2256–2260.
- [13] T. Hines, I. Diez-Perez, J. Hihath, H. Liu, Z. S. Wang, J. Zhao, G. Zhou, K. Müllen, N. Tao, *J. Am. Chem. Soc.* **2010**, 132, 11658–11664.
- [14] During the course of our study, a report of the parent hexayne Py[6] appeared in Chinese, see Ref. [10b]. The details provided are vague, but the molecule was reported as very unstable.
- [15] M. Komatsu, S. Takamatsu, M. Uesaka, S. Yamamoto, Y. Ohshiro, T. Agawa, *J. Org. Chem.* **1984**, 49, 2691–2699.
- [16] Y. Guan, M. P. López-Alberca, Z. Lu, Y. Zhang, A. A. Desai, A. P. Patwardhan, Y. Dai, M. J. Vetticatt, W. D. Wulff, *Chem. Eur. J.* **2014**, 20, 13894–13900.
- [17] G. Bélanger, M. Doré, F. Ménard, V. Darsigny, *J. Org. Chem.* **2006**, 71, 7481–7484.
- [18] M. X.-W. Jiang, M. Rawat, W. D. Wulff, *J. Am. Chem. Soc.* **2004**, 126, 5970–5971.
- [19] X. Nie, G. Wang, *J. Org. Chem.* **2006**, 71, 4734–4741.
- [20] W. Chodkiewicz, P. Cadiot, *C. R. Chim.* **1955**, 241, 1055–1057.
- [21] A. S. Hay, *J. Org. Chem.* **1962**, 27, 3320–3321.
- [22] G. Eglinton, A. R. Galbraith, *Chem. Ind.* **1956**, 737–738.
- [23] E. Merkul, D. Urselmann, T. J. J. Müller, *Eur. J. Org. Chem.* **2011**, 238–242.
- [24] Due to insufficient quantities of material, Py\*[8] could not be analyzed by DSC, and decomposition is reported based on open measurement in an open capillary.
- [25] T. Luu, E. Elliott, A. D. Slepko, S. Eisler, R. McDonald, F. A. Hegmann, R. R. Tykwinski, *Org. Lett.* **2005**, 7, 51–54.
- [26] H. Higuchi, N. Hayashi, T. Matsukihira, T. Kawakami, T. Takizawa, J. Saito, K. Miyabayashi, M. Miyake, *Heterocycles* **2008**, 76, 353–380.
- [27] a) M. Koepf, A. Trabolsi, M. Elhabiri, J. A. Wytke, D. Paul, A. M. Albrecht-Gary, J. Weiss, *Org. Lett.* **2005**, 7, 1279–1282; b) T. Tanaka, A. Osuka, *Chem. Soc. Rev.* **2015**, 44, 943–969.
- [28] A. D. Shukla, P. C. Dave, E. Suresh, A. Das, P. Dastidar, *J. Chem. Soc. Dalton Trans.* **2000**, 4459–4463.
- [29] Due to low synthetic yields of Py\*[8], this derivative was not used for coordination experiments with either **11** or **12**.
- [30] N. Jux, *Org. Lett.* **2000**, 2, 2129–2132.
- [31] In noncoordinative solvents such as CH<sub>2</sub>Cl<sub>2</sub> and CHCl<sub>3</sub>, porphyrin **12** forms a dimer, which is clearly observable in the <sup>1</sup>H NMR spectra (see Figures S54 and S55). This dimer is readily cleaved in the presence of a more strongly coordinating ligand, such as pyridine. R. Lippert, Ph.D. thesis, University of Erlangen–Nürnberg, **2013**.

- [32] W. A. Chalifoux, M. J. Ferguson, R. McDonald, F. Melin, L. Echegoyen, R. R. Tykwinski, *J. Phys. Org. Chem.* **2012**, 25, 69–76.
- [33] Gladysz and co-workers have reported on the redox behavior of metal-acetylide derivatives, see: J. Stahl, W. Mohr, L. de Quadras, T. B. Peters, J. C. Bohling, J. M. Martin-Alvarez, G. R. Owen, F. Hampel, J. A. Gladysz, *J. Am. Chem. Soc.* **2007**, 129, 8282–8295.
- [34] M. Franz, J. A. Januszewski, D. Wendinger, C. Neiss, L. D. Movsisyan, F. Hampel, H. L. Anderson, A. Görling, R. R. Tykwinski, *Angew. Chem. Int. Ed.* **2015**, 54, 6645–6649; *Angew. Chem.* **2015**, 127, 6746–6750.
- [35] Z. Cao, B. Xi, D. S. Jodoin, L. Zhang, S. P. Cummings, Y. Gao, S. F. Tyler, P. E. Fanwick, R. J. Curtchley, T. Ren, *J. Am. Chem. Soc.* **2014**, 136, 12174–12183.

Received: September 3, 2016

Published online: October 26, 2016